Reconfigurable PIC Transmitter for Short Reach Applications

A. Kaszubowska-Anandarajah[1], K. Sivapalan[2], E. Martin[2], D. Gutierrez-Pascual[3], F. Smyth[3], J. Braddell[3], P. Lakshmijayasimha[2], P. M Anandarajah[2]
[1]*Connect Centre, Trinity College Dublin, Dublin, Ireland*
[2]*Photonics Systems and Sensing Group, Dublin City University, Dublin, Ireland*
[3]*Pilot Photonics Ltd. Invent Centre, Dublin City University, Dublin, Ireland*
anandara@tcd.ie

Abstract: A novel reconfigurable photonic integrated transmitter, enabling dynamic resource allocation and sharing, is proposed. Architecture, functionality and a deployment scenario are discussed. Preliminary work on machine learning methods for controlling the device are also presented.

1. Introduction

The demand for higher data rates and the continuously growing number of connected devices, exert a lot of pressure on telecommunication networks. In addition, the growing dynamicity of the traffic results in either the need to overprovision the network capacity, to cope with the peak demands, or migrate towards more flexible paradigms that enable assigning the network resources to where they are most needed. Within the network, the access and metro segments are faced with the acute problem of providing the required services, while limiting their CAPEX and OPEX, to ensure profitability to the provider. These parts of the network are mostly heterogeneous in nature, serving residential and business area, providing front- and backhaul services to mobile networks etc. Thus, a single "one-size-fits-all" technology is not expected to meet the diverse requirements. Instead, a suite of solutions, focused on the flexibility, performance, scalability and low cost, that can be optimised for individual scenarios, is desirable.

A promising approach entails the adoption of a flexible, pay as you grow strategy during network deployment. Firstly, such an approach would allow the sharing of resources, between different network sectors, according to current capacity demands. Secondly, it enables a gradual investment in the telecommunication infrastructure, dictated by the growing network demands. From a physical layer perspective, the sharing of the infrastructure can be achieved by employing sliceable bandwidth variable transceivers (SBVTs) [1] that can be configured to best support the changing network conditions. Such devices usually consist of an array of lasers and are capable of generating multiple optical channels/flows that can be independently routed to different destinations [2]. Realisation of SBVTs using photonic integrated circuits (PICs) can bring further benefits, such as lower cost, footprint and energy consumption. Replacing the arrays of individual lasers with a multicarrier source, such as an optical frequency comb (OFC), can enhance the spectral efficiency and reduce the energy consumption of the network.

In this paper, we propose a new reconfigurable-PIC (R-PIC) architecture, consisting of a multicarrier SBVT (MC-SBVT) and an optical cross-connect (OXC) that will enable the dynamic reassignment and sharing of the physical network resources. We describe the architecture and functionality of the device, and also present some preliminary work on the development of machine learning (ML) models for controlling the MC-SBVT.

2. R-PIC architecture and functionality

The architecture of the proposed R-PIC, able to generate six wavelength channels and route them to three different output ports, is shown in Fig. 1(a). It consists of an InP MC-SBVT and a SiN OXC, integrated together. The MC-SBVT includes an externally injected gain-switched laser (EI-GSL) based OFC [3], which generates a series of mutually coherent tones. The OFC is then passively split and injected into an array of semiconductor lasers acting as active demultiplexers (ADs) [4]. ADs not only filter and amplify the desired comb tone, but also act as electro-optic converters (through direct modulation of the AD). The demultiplexed and modulated wavelengths are then coupled into the SiN OXC. Each wavelength can be dynamically switched to any output port using a 1×3 optical switch (OS) and a 6×1 multiplexer. The physical realization of the OS can be achieved with a micro ring resonator (MRR) or a mesh of Mach-Zehnder interferometers (MZI), while the multiplexer is based on an MRR, as shown in Fig. 1(b) [5].

Such an architecture provides complete flexibility and reconfigurability of the network resources, allowing them to be deployed where the demand exists. An example of an application of the R-PIC in a metro aggregation node [6] is illustrated in Fig. 1(c). Here, the capacity of the R-PIC is shared between a residential area, a business campus and a 5G access segment. While each of the areas can experience high peak traffic volumes, these are unlikely to occur at the same time. Thus, static assignment of the resources to different segments is inefficient, requiring overprovisioning, to support the peak capacity demands. Alternatively, by using the R-PIC, the capacity of the transmitter can be flexibly redirected between the segments, as the traffic volumes shift, e.g., from the campus to the residential area as the employees return home from work.

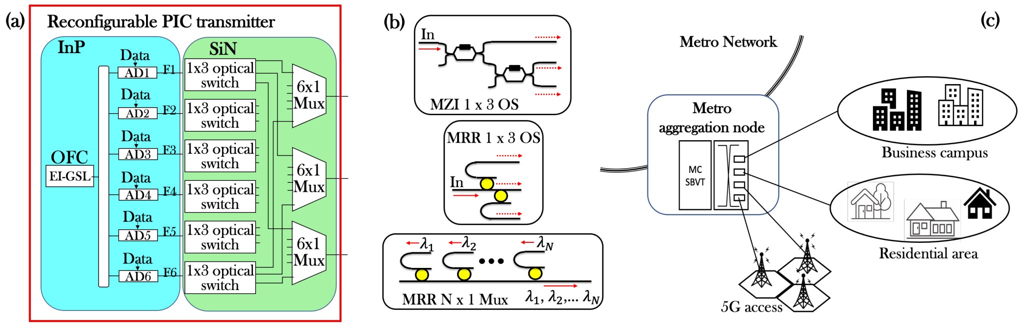

Fig. 1: (a) Block diagram of the R-PIC, (b) schematic of a SiN 1x3 switch and Nx1 multiplexer, (c) metro aggregation node employing R-PIC.

The proposed R-PIC is designed with the maximum flexibility in mind. Use of the EI-GSL together with the AD provides an easy way of varying the wavelength of and spacing between the generated channels. Firstly, the free spectral range (FSR) of the EI-GLS i.e., the baseline channels spacing, can be flexibly adjusted by varying the gain-switching frequency, as shown in Fig. 2 (a) and (b). The second degree of freedom stems from the flexibility of the AD, which can be tuned to the desired wavelength by changing its temperature and/or bias current. In addition, the AD supports asymmetric channel spacings, and offers a supreme finesse, allowing for filtering of very closely spaced lines as shown in Fig. 1(c) and (d). Finally, the data modulation format and the baud rate of the MC-SBVT can be set to match the application requirements and applied by directly modulating the AD [7]. The main constraint here is the bandwidth of the laser and the chirp induced by the direct modulation. Nevertheless, transmission distances of 40-50 km, employing discrete multitone modulation (DMT), has been successfully demonstrated using this method [8]. It is important to note, that the MC-SBVT could also incorporate an external modulator, at the expense of higher loss. The final degree of freedom of the R-PIC stems from the OXC, which allows for any wavelength to be dynamically switched to any output port, and thus any geographical area.

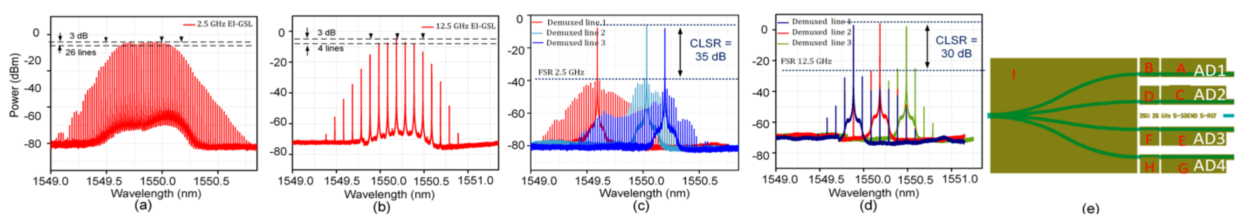

Fig. 2: Optical spectra of OFC with FSR of (a) 2.5 and (b) 12.5 GHz; optical spectra of three demultiplexed lines from OFC with FSR of (c) 2.5 and (d) 12.5 GHz; (e) diagram of an integrated 4-channel active demultiplexer.

3. Calibration and control of R-PIC

While the use of PICs presents many benefits, it also requires overcoming significant challenges, such as achieving a consistent, high yield fabrication, devising fast and scalable testing, developing affordable packaging etc. Moreover, as the number of active sections within the PIC increases, control of such a complex device cannot be efficiently managed using traditional look-up tables or analytical models. Instead, ML models can be used to provide a simple and accurate way for finding the optimum operating points of the device. In this paper, we present some preliminary work carried out on the development of such ML control algorithms for the MC-SBVT. This work focuses on the integrated AD block, as shown in Fig. 2(e). The device consists of a multi-mode interferometer followed by four distributed Bragg reflector (DBR) lasers, acting as ADs. Each AD consists of a gain section (marked as A, C, E and G) and a DBR section (B, D, F and H). The characterisation of the device was started by sweeping the bias currents, applied to both sections of an individual laser (in 2 mA steps), to obtain the wavelength, peak power and side mode suppression ratio (SMSR) maps. Fig. 3 (a-c) show the results obtained from AD1 and similar behaviour was observed for all ADs. The figures show a strong dependence of the chip performance on the bias, with clear mode hops visible in the wavelength maps (marked by the abrupt colour changes), however, the relationship is not a simple one. Furthermore, the behaviour of any laser also depends on the bias currents applied to the other ADs. Fig. 3 (d) shows a change in the wavelength of AD4 (both sections biased at 40 mA), when the current applied to AD1 varies, indicating an existence of thermal and electrical crosstalk between the different sections. Thus, setting a wavelength of any AD cannot be done independently but will require an adjustment of biases of all ADs. Hence, ML is perfectly suited to effectively control such a complex behaviour. We start by developing a ML model for a single AD and then inverting it, to obtain the current settings needed to set the wavelength of the AD to a required value.

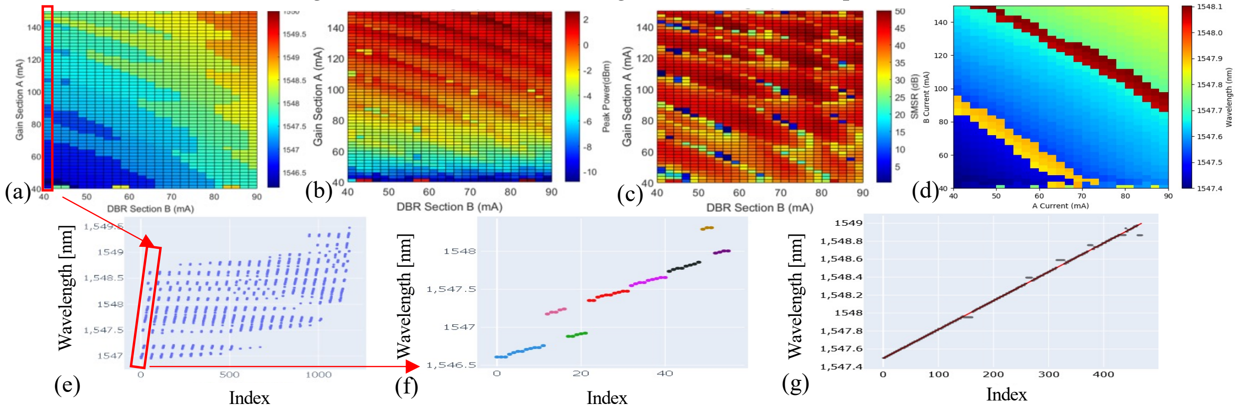

Fig. 3: Tuning maps of AD1 for (a) wavelength, (b) peak power and (c) SMSR; (d) change of the wavelength of AD4 (gain and DBR biased at 40 mA) when the biases of AD1 are swept; (e) flattened AD1 wavelength map, (f) results of DBSCAN clustering performed on the first column of the wavelength map of AD1; (g) comparison between the requested (red line) and the predicted (black dots) wavelength of AD1.

First, we convert the wavelength maps to a 2D plot by indexing all values of the bias applied to the gain and DBR sections, as shown in Fig. 3(e). The figure obtained, consists of 21 groups, each corresponding to a column in the wavelength map (as shown by the red rectangle in Fig. 3 (a) and (e)). The plot shows a piece-wise linear relationship between the wavelength and the current (discontinuities within each group correspond to mode hops). Next, we employ a DBSCAN algorithm [9] to cluster the points within each group, as shown in Fig. 3 (f), and finally use the linear regression to model each cluster. The final step entails the inversion of these linear relationships to predict the bias currents required to set an AD to a desired wavelength (i.e. control the PIC). We tested the accuracy of the method over 570 wavelengths between 1547.5 and 1549 nm by comparing the requested and the predicted wavelength. The results, plotted in Fig. 3 (g), show a very high accuracy of the mode, however there are several values that cannot be set correctly. The reason is that in the verification we used values from only one column in the wavelength map (1 out of 21 clusters), which means that certain wavelengths cannot be achieved. To improve the accuracy, the operation of the predictor needs to be extended to work with all 21 clusters. Furthermore, at present the algorithm only considers the wavelength data and neglects the impact of crosstalk between the different ADs. Thus, the next step is to develop additional layers of the control that will take into consideration the remaining data gathered during the calibration i.e., the peak power and the SMSR and the impact of the aforementioned crosstalk.

4. Conclusions

A novel architecture of an R-PIC for short reach applications, delivering a fully flexible wavelength, output port assignment, and allowing dynamic sharing of the physical resources between different network segments, has been proposed. The combination of an OFC, ADs and the SiN OXC delivers a suite of benefits, including reduced cost, improved spectral and energy efficiency, and small footprint. We have also presented some preliminary work carried out on the development of the first, to the best of our knowledge, ML model that can be employed to control an active PIC. The model converts the wavelength tuning maps to sets of linear functions, which can be easily inverted to obtain the bias currents to set the desired operating point of the AD. In the future, this model will be expanded to include other characteristics of the device, such as peak power and SMSR, as well as the impact of crosstalk between different sections of the device.

Acknowledgments: This work is supported by DTIF (DT20180268), Science Foundation Ireland (15/CDA/3640), and SFI/European Regional Development Fund (13/RC/2077_P2).

5. References

[1] L. Nadal et al., "SDN-Enabled S-BVT for Disaggregated Networks: Design, Implementation and Cost Analysis," IEEE J Lightwave Technol, 11, pp. 3037-3043, (2020)
[2] E. Riccardi et al., "Sliceable bandwidth variable transponders for elastic optical networks: The idealist vision," in Fotonica AEIT Italian Conference on Photonics Technologies, pp. 1-4, (2015)
[3] M. Pascual, et. al., "InP photonic integrated externally injected gain switched optical frequency comb," Opt. Lett. 42, pp.: 555-558 (2017)
[4] P. Lakshmijayasimha, et al., "Characterization of a multifunctional active demux for frequency combs", Opt Laser Technol, 134 (2021)
[5] D. J. Blumenthal, et.al., "Silicon Nitride in Silicon Photonics," in Proceedings of the IEEE, vol. 106, no. 12, pp. 2209-2231, (2018)
[6] https://zenodo.org/record/2586698#.YYPEYb3P2WA
[7] A. Kaszubowska-Anandarajah, et. al., "A multifunctional demultiplexer for optical frequency combs in broadband access networks," SPIE Photonics West, pp.:11307-11, (2020)
[8] S. Ahmad et. al., "Active demux-enabled direct mod. DMT transmission using OFCs for DCIs", J. Light. Technol., 17, pp.: 5468-5473 (2021)
[9] https://www.kdnuggets.com/2020/04/dbscan-clustering-algorithm-machine-learning.html